Double-Cubane [8Fe9S] Clusters: A Novel Nitrogenase-Related Cofactor in Biology

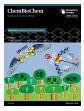

Jae-Hun Jeoung,[b] Berta M. Martins,[b] and Holger Dobbek*[a]

Three different types of electron-transferring metallo-ATPases are able to couple ATP hydrolysis to the reduction of low-potential metal sites, thereby energizing an electron. Besides the Fe-protein known from nitrogenase and homologous enzymes, two other kinds of ATPase with different scaffolds and cofactors are used to achieve a unidirectional, energetic, uphill electron transfer to either reduce inactive Co-corrinoid-containing proteins (RACE-type activators) or a second iron-sulfur cluster-containing enzyme of a unique radical enzymes family (archerases). We have found a new cofactor in the latter enzyme family, that is, a double-cubane cluster with two [4Fe4S] subclusters bridged by a sulfido ligand. An enzyme containing this cofactor catalyzes the ATP-dependent reduction of small molecules, including acetylene. Thus, enzymes containing the double-cubane cofactor are analogous in function and share some structural features with nitrogenases.

1. Introduction

Most electron transfer reactions involve the overall transfer from an electron donor/acceptor couple with negative midpoint potential to one with a positive midpoint potential, thermodynamically downhill. But it requires electrons of very low redox potentials to reduce some unreactive compounds and thus transferring electrons against the thermodynamic potential gradient is warranted to generate these energetic electrons. This requires a source of energy, which may, in relation to the source of the electrons be internal or external.

Such an internal source of electrons is found in electron bifurcation mechanisms, such as in the quinone-based bifurcation of the Q cycle in the cytochrome bc_1-complex or the recently discovered flavin-based bifurcation found in a steadily increasing number of energy converting pathways in anaerobic microorganisms.[1–6] In electron bifurcation mechanisms, the thermodynamic downhill electron transfer of one electron is coupled to the thermodynamic uphill electron transfer of a second electron.

In contrast to using an internal energy source, external sources bring a second type of source into the process. In terms of sustainability, the ideal source may be light, which is used to energize electrons in photosynthesis. But also the universal current of energy in our cells, adenosine triphosphate (ATP), whose energy-rich phosphoanhydride bonds may be hydrolyzed to drive a plethora of different physiological processes, is a driver for electron transfer reactions – creating a process that, overall, reverses oxidative phosphorylation[7] (Table 1).

1.1. Electron-transferring metallo-ATPases

To date, three different types of metallo-ATPases coupling electron transfer to the hydrolysis of ATP are known: 1) systems homologous to nitrogenase reductase, 2) the RACE-type activators and 3) the archerases.

Nitrogenase catalyzes the ATP-dependent reduction of dinitrogen (N_2) to ammonia (NH_3).[8,9] Systems homologous to nitrogenase are involved in bacteriochlorophyll and coenzyme F_{430} biogenesis and have the same principal composition as nitrogenase, with a dimeric metallo-ATPase (the Fe-protein in nitrogenases) driving the reduction of the catalytic component.[10]

The Fe-protein belongs to a group of P-loop ATPases with a synapomorphic KGG motif in the Walker A motif, called Mrp/MinD-family.[11] Characteristic of this NTPase family is a coupling of nucleotide binding and hydrolysis to conformational changes within the dimer interface. In case of the Fe-protein, this allows to modulate the properties of its [4Fe4S] cluster, which is positioned in the dimer interface and moves towards and away from the next potential electron acceptor, in complexes of the Fe-protein with its catalytic partner.[12,13]

The mechanism of ATPase-coupled electron transfer from the Fe-protein to the MoFe-protein has been studied in some detail.[14] The Fe-protein, loaded with two ATP molecules, forms a complex with the MoFe-protein. Electron transfer occurs before ATP hydrolysis and an internal electron transfer within the MoFe-protein, triggered by the Fe-protein precedes a transfer from the Fe-protein to the MoFe-protein - a mechanism termed „deficit spending“ electron transfer.[15,16] Only after the electron transfer from the Fe-protein to the MoFe-protein, the

[a] Prof. Dr. H. Dobbek
Institut für Biologie, Strukturbiologie/Biochemie
Humboldt-Universität zu Berlin
Unter den Linden 6, 10099 Berlin (Germany)
E-mail: holger.dobbek@hu-berlin.de
[b] Dr. J.-H. Jeoung, Dr. B. M. Martins
Institut für Biologie, Strukturbiologie/Biochemie
Humboldt-Universität zu Berlin
Unter den Linden 6, 10099 Berlin (Germany)

This article is part of a Special Issue on Nitrogenases and Homologous Systems.

Table 1. ATP-driven reductive systems.

System (e^--acceptor/ e^--donor)	ATPase class	ATP/ e^-	Cofactors (e^--acceptor/ e^--donor)	Biological function
MoFe-protein/ Fe protein	MinD	2	[8Fe7S] [Mo7Fe9SC]/ [4Fe4S]	Reduction of N_2 to NH_3
DPOR[a] ChlNB/ ChlL	MinD	2	[4Fe4S]/ [4Fe4S]	Reduction of double bond in Pchlide[g]
COR[b] BchlNB/ /BchlL	MinD	2	[4Fe4S]/ [4Fe4S]	Reduction of double bond in Bchlide[h]
CoFeSP[c]/ RACo[d]	ASKHA	1	Corrinoid/ [2Fe2S]	Methyltransfer
BcrBC/ BcrAD	ASKHA	1	2 [4Fe4S]/ [4Fe4S]	Reduction of aromatic rings of benzoyl-CoA
HAD[e] enzyme/ activator	ASKHA	1	[4Fe4S]/ [4Fe4S]	Dehydration of (*R*)-2-hydroxy-acyl-CoA
DCCP/ DCCPR	ASKHA	nd[f]	[8Fe9S]/ [4Fe4S]	unknown

[a] dark operative protochlorophyllide oxidoreductase. [b] chlorophyllide oxidoreductase. [c] Corrinoid iron-sulfur protein. [d] Reductive activator of CoFeSP. [e] 2-hydroxyacyl-CoA dehydratases. [f] not determined. [g] protochlorophyllide. [h] bacteriochlorophyllide.

Fe-protein hydrolyzes ATP, likely triggering complex dissociation.[15] Conformational changes in the Fe-protein not only modulate the environment of its [4Fe4S] cluster, but have also to trigger the internal electron transfer within the MoFe-protein. Thus, ATPase-coupled electron transfer has not only to energize an electron but also to orchestrate electron transfer, e.g. to make it unidirectional. Interestingly, Fe-protein has itself the ability to reduce small molecules such as CO_2.[17–19]

A second type of ATP-driven electron transfer is found in the reductive activators of corrinoid-containing enzymes, RACE-type ATPases for short.[20–23] RACE-type ATPases support the activity of Co-corrinoid containing enzymes involved in methyl transfer reactions, for which their Co-ion is cycling between the methylated Co^{3+} and the Co^{+} state. The latter is prone to oxidation to the inactive Co^{2+} state, which the RACE-type ATPases reduce back to the active Co^{+} state at the expense of ATP. RACE-type ATPases occur in anaerobic bacteria and archaea, including acetogens.[23]

Unlike the Fe-protein, RACE-type activators are not members of the abundant P-loop NTPases, but belong to the ancient ASKHA-type ATPases, where ASKHA stands for the prototypical members of this class, acetate and sugar kinases, heat shock cognate 70 and actin. The electron donor in the RACE-ATPase is a [2Fe2S] cluster harbored in plant-type [2Fe2S]-cluster ferredoxin type domain, which is flexibly linked to the ATPase core.[23] Complex formation between the ATPases and its cognate partner depends on the oxidation of the Co-ion and a direct interaction between the corrinoid cofactor and the ATPases was detected in solution and in a crystal structure.[23–25]

1.2. Benzoyl-CoA reductases and 2-hydroxyacyl-CoA dehydratases

A third type of ATP-dependent electron transferases is found in the ATP-dependent benzoyl-CoA reductases and 2-hydroxyacyl-CoA dehydratases, which are forming a distinct radical enzyme family with only [4Fe4S] clusters as prosthetic groups.[26] So far, these and homologous enzymes of the FldB/C sequence family were found to catalyze two different types of reactions, the reduction of the aromatic rings of benzoyl-CoA to a cyclic dienoyl-CoA and the dehydration (*syn*-elimination of water) from 2-hydroxyacyl-CoA esters - two mechanistically demanding reactions.[26–28]

The reduction of an aromatic ring has the challenge to break the stable resonance structure, which is overcome in Birch-type reactions using a very strong reducing agent.

While the dehydration of 3-hydroxyacyl-CoA esters are facile and well known from beta-oxidation of fatty acids, 2-hydroxyacyl-CoA esters lack the required acidic proton at C3.[29] To overcome this mechanistic challenge, the enzymes induce an umpolung of the substrate carbonyl by generating a ketyl-radical anion intermediate, in which the carbonyl atom becomes nucleophilic, inducing the elimination of the hydroxyl group at C2, followed by a deprotonation of the generated enoxy radical.[30,31] As a dehydration is an overall non-redox reaction, the electron is recycled and the ATPase only acts as an activator for the overall reaction. In contrast, benzoyl-CoA reductases require two electrons per turnover, of which the first likely also generates a ketyl-radical anion before breaking down the aromaticity of benzoyl-CoA.[26]

The catalytic systems are composed of the two principal components, the electron donor, a dimeric ASKHA-type ATPase and the catalytic unit, formed by two homologous subunits, each containing a [4Fe4S] cluster that bind the CoA-substrate and harbor the active site. Complexes between the two components may be stable (some benzoyl-CoA reductases) or may depend on the nucleotide bound in the ATPase module, as shown for 2-hydroxyisocaproyl-CoA dehydratase.[32,33]

The crystal structures of both components of 2-hydroxyisocaproyl-CoA dehydratase (HadBC and HadI), and of the ATPase from 2-hydroxyglutaryl-CoA dehydratase (HgdC) have been determined.[33–35]

The dimeric ATPases harbor an ATP-binding site within an ASKHA fold, which they combine with a [4Fe4S] cluster bound in the dimer interface.[33,34] One helix of each subunit is pointing towards the [4Fe4S] cluster with a helix-cluster-helix angle of 105°. As this is likely to change during complex formation and electron donation, the helix-cluster-helix arrangement has been likened to a bow, shooting the electron, like an arrow by a sudden change in the angle. This analogy has given rise to the name archerases for these electron-transfer ATPases.[36]

The [4Fe4S] cluster of archerases is rapidly reduced either using the physiological reductants ferredoxin and flavodoxin or the non-physiological reductants dithionite and Ti^{III}-citrate.[37,38] An excess of Ti^{III}-citrate generates the inactive two-electron reduced all-ferrous state $[4Fe4S]^0$.[39] Thus, while relying on an unrelated ATPase-fold, the archerases show obvious parallels to

the Fe-protein of nitrogenases, both in the position of the [4Fe4S] cluster in a dimer interface, and in the formation of the all-ferrous state.

The crystal structure of 2-hydroxyisocaproyl-CoA dehydratase (HadBC) revealed that each subunit coordinates one [4Fe4S] cluster, each coordinated by three cysteine residues, leaving a unique Fe-ion in the cluster without protein ligand.[35] Whereas in the substrate binding subunit HadB a water ligand binds to the unique Fe, a sulfhydryl-ligand binds the unique Fe in the accessory subunit HadC. Binding of 2-hydroxyisocaproyl-CoA replaces the water ligand at the unique Fe-ion to which instead the carbonyl-oxygen of the CoA moiety is binding. In contrast, substrate doesn't bind in HadC and its [4Fe4S] cluster likely acts as a storage place for the energetic electron required to generate the ketyl-radical anion.

2. The FldB/C sequence family

We inspected the various amino acid sequences with homology to FldB/C. To display this variability, we constructed a sequence similarity network from the sequences stored with the InterPro entry IPR010327, which consisted at the time of 1,436 sequences homologous to benzoyl-CoA reductases B/C (BcrB/C) and the α/β subunit of atypical dehydratases (HadB/C) (Figure 1).[40] Sequences originate from the genomes of bacteria and archaea, including firmicutes, spirochaetes, actinobacteria, enterobacteria, delta-proteobacteria, and euryarchaeota. Depending on the cutoff level defining similarity, we may discriminate five larger and several smaller clusters.

Sequences with cluster I are most varied in terms of sequence length, ranging from 420 to 1800 amino acids. Most of the longer sequences are fusions between catalytic dehydratase/reductase-type subunits and ATP-dependent archerases.

Sequences in cluster II contain on average about 380 amino acids and include the α-subunits of benzoyl-CoA reductases and the β-subunits of atypical dehydratases. These subunits likely support the function of the catalytic subunits, as found for 2-hydroxyisocaproyl-CoA dehydratase.[35]

Cluster III contains the catalytic subunits of benzoyl-CoA reductases (β-subunits) and atypical dehydratases (α-subunits). Sequences are on average longer than their supporting partner subunits in cluster II. Both, the sequences of cluster II and cluster III share conserved motifs with 3×Cys to bind a [4Fe4S] cluster.

Mostly associated to sequence cluster II, comprising proteins with 380–420 amino acids, are the sequences in cluster IV. The primary distinction of these sequences from cluster II is a set of conserved cysteine residues, making up a 7-Cys motif $CX_{19}CX_{18\text{-}19}CX_{29}CX_{166\text{-}170}CX_{32\text{-}34}CX_{32}C$. Among these proteins are CHY_0487 from *Carboxydothermus hydrogenoformans* and YjiM from *Escherichia coli*.

YjiM is with 388 amino acids one of the shorter proteins of cluster IV and is associated with YjiL, which is homologous to the ATP-dependent archerases. CHY_0487 from *C. hydrogenoformans* (named $DCCP_{Ch}$) is with 421 amino acids a member of the group of long sequences within the cluster. $DCCP_{Ch}$ is associated with CHY_0488 (named DCCP-R_{Ch}), which was annotated to be an ATP-dependent activator for CoA-specific enzymes. This association of the two genes, also found for the other enzymes of cluster IV, is in line with a two-component system, catalyzing the ATP-dependent electron transfer from one protein, with the seven-Cys containing enzyme being the electron acceptor.

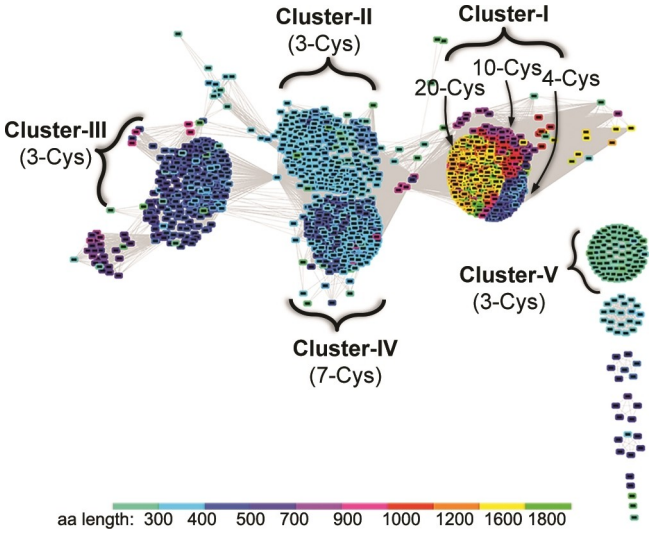

Figure 1. Sequence-similarity clustering. Sequence-similarity clustering of the InterPro entry IPR010327 using the EFI-EST server identifies five larger sequence clusters (I–V).[41] The InterPro entry contains sequences encoding the alpha and beta subunits of 2-hydroxyacyl-CoA dehydratases and ATP-dependent benzoyl-CoA reductase (FldB/C, HgdA/B and BcrB/C). Sequence network was visualized using Cytoscape (v3.3.0)[42] and is color coded according to the length of sequences.

2.1. $DCCP_{Ch}$ and DCCP-R_{Ch}

We overproduced $DCCP_{Ch}$ and DCCP-R_{Ch} from *C. hydrogenoformans* in *E. coli*. Both proteins are of a brown color when prepared under anoxic conditions, indicative of the presence of iron-sulfur clusters.[40]

$DCCP_{Ch}$ and DCCP-R_{Ch} form homodimers in solution. While sodium dithionite is able to reduce the [4Fe4S] cluster in DCCP-R_{Ch}, observed by a diminished absorbance at 420 nm, the Fe/S cluster in $DCCP_{Ch}$ shows no change in absorbance when thionine-oxidized $DCCP_{Ch}$ is incubated with sodium dithionite or Ti^{III}-citrate. But when in addition to DCCP-R_{Ch} also Mg-ATP is added to the solution, the Fe/S cluster in $DCCP_{Ch}$ becomes reduced. Thus, the two proteins form an ATP-dependent two-component system.

$DCCP_{Ch}$ was crystallized under strictly anoxic conditions and its structure confirms the homodimeric arrangement (Figure 2). Each subunit is composed of two domains, an N-terminal (1–193 aa) and a C-terminal (194–420 aa) domain, with the Fe/S cluster bound between the two domains. Both domains have a similar-type of open fold (Rossman-fold) with a four-stranded beta-sheet covered on both sides by α-helices and revealed a

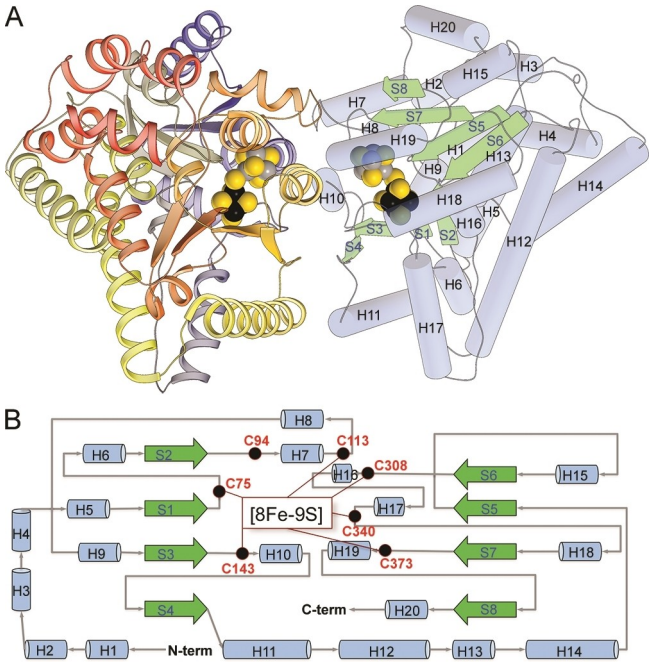

Figure 2. Overall structure of DCCP. A) Homodimeric overall structure of DCCP (PDB ID: 6ENO,[40]). One subunit (cartoon) is colored from red (N-terminus) via yellow to blue (C-terminus), while the other subunit is depicted in α-helices (light blue cylinder) and β-strands (green block-arrow). The DCC is shown as spheres with different colors for iron: black (α-subcluster) and gray (β-subcluster). Sulfur atoms are golden colored. B) Topology diagram showing the secondary structure elements using the same colors as in A. Black circles indicate the positions of the conserved 7-Cys residues.

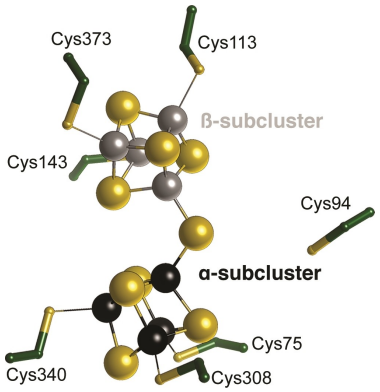

Figure 3. Double cubane cluster (DCC). Conserved 7-Cys residues with the six coordinating Cys ligands and the seventh Cys (Cys94) next to the DCC. Iron atoms are color-coded as in Figure 2 and carbon atoms shown in dark green.

sequence identity of 22%, indicative of homology between the domains and a common ancestor from which the gene encoding $DCCP_{Ch}$ evolved by gene-duplication.

2.2. The double-cubane cluster (DCC)

At its heart $DCCP_{Ch}$ carries an unusual Fe/S cluster with a composition of a [8Fe:9S] cluster (Figure 3). The cluster is composed of two juxtaposed [4Fe4S] clusters, which are linked by a sulfide ligand, resulting in a $[\{Fe_4S_4(SCys)_3\}_2(\mu_2\text{-}S)]$ cluster. The cluster is termed double-cubane cluster (DCC), a name we also used to refer to the enzymes.

The DCC is coordinated by six cysteine residues, all of which are part of the characteristic 7-Cys motif of cluster IV sequences (Figure 1). The cysteine residues do not coordinate two out of the eight Fe ions, which are the nearest Fe ions between the two cubanes and are linked by a μ_2-sulfido ligand. The two [4Fe4S] subclusters in the DCC are rotated against each other, with shortest Fe–Fe distances between the two subclusters of 3.7 Å. The shortest Fe–Fe distance between the two DCCs in the homodimer is only 14 Å, which would allow a rapid inter-DCC electron transfer.

An [8Fe:9S] cluster had not yet been observed in any other enzyme and therefore extends natures repertoire of biological cofactors. But unlike the biological perspective, [8Fe:9S] clusters of very similar structure have already been synthesized and reported.[43]

$DCCP_{Ch}$ is the first protein reported containing a DCC. While [4Fe4S] clusters are found not only alone, but also as building blocks for active site cofactors, these cofactors contain additionally either a 2Fe-site (H cluster in [Fe,Fe] hydrogenases), a 2Ni-site (A cluster in acetyl-CoA synthase) or a heme group (siroheme in sulfite and nitrite reductases), not an additional [4Fe4S]-unit as we see in $DCCP_{Ch}$.[40,44–50]

On the other hand, cofactors containing complex Fe/S clusters with over four Fe ions are well established and are one characteristic of the nitrogenase system (Figure 4). Both the M cluster in FeMo-nitrogenase and the FeV-nitrogenase have seven Fe ions,[54,58] but their overall arrangement is not that of two neighboring [4Fe4S] clusters and contain not one but three μ_2-bridging sulfido-ligands, making it more tightly fused. More similar in structure to the DCC is the P cluster. But while the P clusters shares with the DCC the composition of eight Fe ions, it contains two sulfur ions less than the DCC, is bound in the interface between two subunits and is again more compact than the DCC.

Interestingly, two closely spaced [4Fe4S] clusters, like the DCC are also the supposed starting material to form the P cluster. Specifically, a precursor state of the P cluster termed P* cluster, is likely similar to the DCC and, excitingly it is also catalytically active in catalyzing the reduction of acetylene and hydrazine, and the useful reduction of CO and CN to alkanes and alkenes.[59,60]

Thus, the DCC shares similarities with the nitrogenase cofactors and even more so with intermediate maturation-states of these cofactors. Furthermore, all of these complex Fe/S clusters receive electrons from an ATP-dependent reductase, which injects electrons from a [4Fe4S] cluster as electron donor.

Although new to biology, DCCs were already prepared by synthetic inorganic chemists and a first DCC, in which both [4Fe4S] clusters are bridged by a μ-sulfido-ligand, was reported by Stack, Carney and Holm in 1989.[43] The μ-sulfido-containing

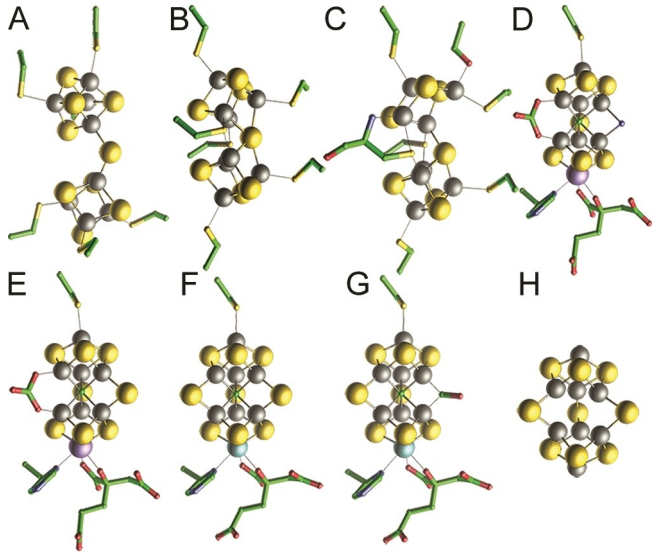

Figure 4. Comparison of complex Fe/S clusters. A) DCC [8Fe:9S] (6ENO,[40]). B) Reduced P cluster [8Fe:7S] (5KOH,[51]). C) Oxidized P cluster [8Fe:7S] (2MIN,[52]). D) Nitrogen-bound FeV cofactor cluster [V:7Fe:7S:C:N:CO_3] (6FEA,[53]). E) FeV cofactor cluster [V:7Fe:7S:C:CO_3] (5 N6Y,[54]). F) FeMo cofactor (M cluster) in nitrogenase [Mo:7Fe:9S:C] (3 U7Q,[55]). G) CO-bound FeMo cofactor [Mo:7Fe:9S:C:CO] (4TKV,[56]). H) Precursor of M cluster [8Fe:9S] (3PDI,[57]). Atoms colored: Fe (dark gray), Mo (cyan), V (light purple), S (gold), O (red), N (blue), and C (green).

variant and other DCCs with other bridging ligands have been studied since.[61,62]

The analysis of the synthetic DCCs helps us to understand what we could expect as properties of the DCC. Most remarkably and likely of functional relevance, DCCs display a peculiar redox chemistry.[43] As long as two [4Fe4S] clusters are well separated, they act as individual and independent entities, displaying the same midpoint potential if they have the same environment. But, once the two [4Fe4S] clusters approach each other, their redox transitions depend upon each other and thus are coupled. Inorganic DCCs in organic solvents display very low reduction potentials ($E_{1/2} < -1$ V *vs.* Ag/$AgNO_3$) with two transitions separated by 190–220 mV.[62]

2.3. Potential substrates

The DCCPs are so far only characterized by their cofactor content, but not by their physiological function. Thus, we can only infer potential functions from the structure and the reactivity of the DCC with nonphysiological substrates.

Both types of enzymes with similarity to $DCCP_{Ch}$, benzoyl-CoA reductases and atypical dehydratases, convert CoA-esters, making a CoA ester the first guess as a potential substrate. But CoA esters are large and the structure of isocaproyl-CoA dehydratase in complex with its substrate shows the space they require to bind.[35] While the isocaproate moiety binds near the [4Fe4S] cluster, with the carbonyl-oxygen of the thioester group coordinating the open coordination side of the unique iron of the [4Fe4S] cluster, the CoA is accommodated within a funnel-shaped substrate-binding cavity with a wide opening to house the phosphorylated ADP-moiety of CoA.

The structures of $DCCP_{Ch}$ and isocaproyl-CoA dehydratase superimpose very well, placing the metal clusters at equivalent positions (Figure 5). While the overall fold shows the same architecture, the funnel-shaped CoA-binding channel of isocaproyl-CoA dehydratase is missing in $DCCP_{Ch}$. Four helices, originating from an N-terminal extension of $DCCP_{Ch}$ compared to isocaproyl-CoA dehydratase, are occluding the channel and leave little space for substrates to enter.

At the site of the wide channels of isocaproyl-CoA dehydratase, we find two narrow channels leading to the DCC (Figure 5). Both channels are too narrow to take up a CoA ester, making it unlikely for $DCCP_{Ch}$ to bind CoA esters unless the structure undergoes larger conformational changes, which appears unlikely given the rather compact fold of $DCCP_{Ch}$. Interestingly, the narrow substrate channels are not necessarily common to all DCCPs. YjiM, a potential DCC-containing enzyme from *E. coli* sharing the seven-Cys motif, lacks the N-terminal extension found in $DCCP_{Ch}$, rendering a CoA-ester substrate more likely for this enzyme.

Given 1) the small size of the channel in $DCCP_{Ch}$ and 2) the mentioned analogies to nitrogenase, a role in small-molecule activation by the enzyme appears likely and we explored its reactivity with different small molecules.[40]

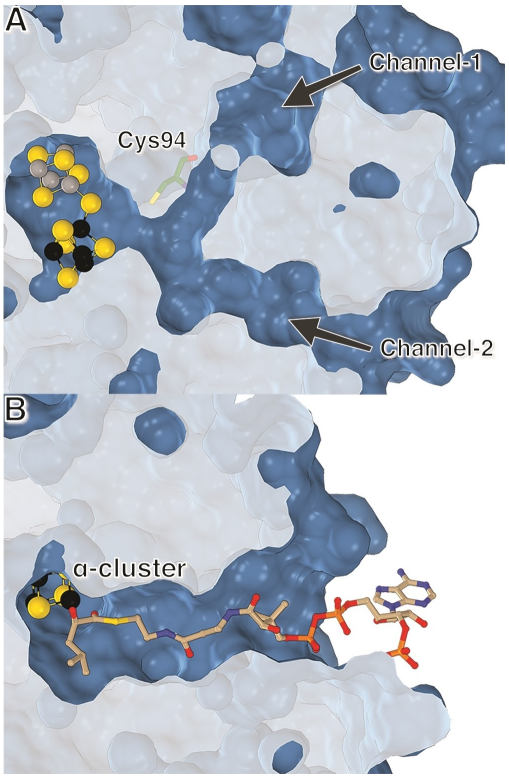

Figure 5. Side-by-side view of channels in DCCP (6ENO,[40]) (A) and (*R*)-2-hydroxyisocaproyl-CoA dehydratase (PDB id: 3O3 N,[35]) (B). Black arrows indicate the two channels in DCCP. (*R*)-2-hydroxyisocaproyl-CoA is represented by sticks with light brown carbon atoms. DCC is colored same as Figure 2. Iron atoms of the [4Fe4S] cluster of (*R*)-2-hydroxyisocaproyl-CoA dehydratase are colored in black. Sulfur atoms are drawn in gold.

$DCCP_{Ch}$, in the presence of DCCP-R_{Ch}, Mg-ATP and sodium dithionite, rapidly reduces acetylene to ethylene, reaching a k_{obs} of 4.3 min^{-1}. Reduction of acetylene requires both components and is strictly Mg-ATP dependent. Indeed, the rate of acetylene reduction is similar to the rate of ATP hydrolysis determined under the given conditions (k_{obs} of 3.2 min^{-1}), showing that the ATP-dependent reduction of $DCCP_{Ch}$ by DCCP-R_{Ch} is either rate-limiting or coupled to substrate turnover. The tendency of the DCC to interact with small molecules is further supported by its inhibition. CO and potassium cyanide reversibly inhibit acetylene reduction by $DCCP_{Ch}$, suggesting that both inhibitors bind close to or directly at the DCC.

Its ability to reduce acetylene, as well as its tendency to be inhibited by CO and cyanide, further emphasize the parallels between the DCCPs and the nitrogenase systems.

3. Outlook

As the structure of $DCCP_{Ch}$ defines the cysteine residues coordinating the DCC, it appears likely that proteins containing the same characteristic sequence motif with these six cysteine residues also contain a DCC. This applies at least to the sequences of cluster IV, including enzymes of different length and different bacteria.

As with other cofactors, the question arises whether the DCC is only associated with one kind of function, like the C cluster of CODHs, the A cluster of acetyl-CoA synthases or the P cluster and FeMo/FeV cofactors of nitrogenases or if it may be associated with different conversions and may support entirely different functions. Based on sequence similarities and modelling on the $DCCP_{Ch}$ structure, we believe that the DCC supports conversions of different substrates and that at least three different classes of DCCPs may exist.

$DCCP_{Ch}$, may exemplify class-I whose active site appears to be primed for the activation and turnover of small molecules. The DCCP from *E. coli*, YjiM may represent class II. While only 33 amino acids shorter in sequence than $DCCP_{Ch}$, YjiM lacks the channel closing helices and may therefore, like benzoyl-CoA reductase and atypical dehydratases, bind and convert a CoA ester or another larger substrate.

While the first and second class share the complete seven-Cys motif, sequences of class III of potential DCCPs lack one cysteine residue in the motif. While the six cysteine residues coordinating the DCC are present, a conserved cysteine residue of classes I and II resting close to the opening above the DCC, is missing. Enzymes of class III and their reductase are encoded in one polypeptide of about 550 amino acids. These sequences are abundant among firmicutes, including pathogens such as *Clostridium botulinum*.

Thus, the underlying question, if the DCC is restricted to one function or may serve different physiological functions is yet to be established. We believe that we are just at the beginning to uncover more than one potential role of DCCs.

Acknowledgements

Funded by the Deutsche Forschungsgemeinschaft (DFG, German Research Foundation) under Germany's Excellence Strategy – EXC 2008 – 390540038" – UniSysCat and by DFG grant DO 785/8-1 as part of DFG SPP 1927).

Conflict of Interest

The authors declare no conflict of interest.

Keywords: iron/sulfur cluster · small-molecule activation · ATP · electron transfer · nitrogenase

[1] P. Mitchell, *FEBS Lett.* **1975**, *59*, 137–139.
[2] G. Herrmann, E. Jayamani, G. Mai, W. Buckel, *J. Bacteriol.* **2008**, *190*, 784–791.
[3] F. Li, J. Hinderberger, H. Seedorf, J. Zhang, W. Buckel, R. K. Thauer, *J. Bacteriol.* **2008**, *190*, 843–850.
[4] R. K. Thauer, A.-K. Kaster, H. Seedorf, W. Buckel, R. Hedderich, *Nat. Rev. Microbiol.* **2008**, *6*, 579–591.
[5] W. Buckel, R. K. Thauer, *Biochim. Biophys. Acta* **2013**, *1827*, 94–113.
[6] W. Buckel, R. K. Thauer, *Chem. Rev.* **2018**, *118*, 3862–3886.
[7] A. Szent-Gyorgyi, *Introduction to a Submolecular Biology*, Academic Press **1960**.
[8] B. M. Hoffman, D. Lukoyanov, Z.-Y. Yang, D. R. Dean, L. C. Seefeldt, *Chem. Rev.* **2014**, *114*, 4041–4062.
[9] N. S. Sickerman, Y. Hu, M. W. Ribbe, *Methods Mol. Biol.* (Eds.: M. W. Ribbe, Y. Hu) **2019**, pp. 3–24.
[10] J. Moser, G. Layer, *Metalloproteins* (Ed.: Y. Hu), Springer New York, New York, NY **2018**, pp. 25–35.
[11] D. D. Leipe, Y. I. Wolf, E. V. Koonin, L. Aravind, *J. Mol. Biol.* **2002**, *317*, 41–72.
[12] M. M. Georgiadis, H. Komiya, P. Chakrabarti, D. Woo, J. J. Kornuc, D. C. Rees, *Science* **1992**, *257*, 1653–1659.
[13] H. Schindelin, C. Kisker, J. L. Schlessman, J. B. Howard, D. C. Rees, *Nature* **1997**, *387*, 370–376.
[14] L. C. Seefeldt, J. W. Peters, D. N. Beratan, B. Bothner, S. D. Minteer, S. Raugei, B. M. Hoffman, *Cu. Op. Chem. Biol.* **2018**, *47*, 54–59.
[15] S. Duval, K. Danyal, S. Shaw, A. K. Lytle, D. R. Dean, B. M. Hoffman, E. Antony, L. C. Seefeldt, *Proc. Natl. Acad. Sci. USA* **2013**, *110*, 16414–16419.
[16] K. Danyal, D. R. Dean, B. M. Hoffman, L. C. Seefeldt, *Biochemistry* **2011**, *50*, 9255–9263.
[17] J. G. Rebelein, M. T. Stiebritz, C. C. Lee, Y. Hu, *Nat. Chem. Biol.* **2017**, *13*, 147–149.
[18] C. C. Lee, M. T. Stiebritz, Y. Hu, *Acc. Chem. Res.* **2019**, *52*, 1168–1176.
[19] L. A. Rettberg, W. Kang, M. T. Stiebritz, C. J. Hiller, C. C. Lee, J. Liedtke, M. W. Ribbe, Y. H. Y. Hu, *mBio* **2019**, *10*, DOI 10.1128/mBio.01497–19.
[20] A. Siebert, T. Schubert, T. Engelmann, S. Studenik, G. Diekert, *Arch. Microbiol.* **2005**, *183*, 378–384.
[21] T. Ferguson, J. A. Soares, T. Lienard, G. Gottschalk, J. A. Krzycki, *J. Biol. Chem.* **2008**, *284*, 2285–2295.
[22] A. Schilhabel, S. Studenik, M. Vodisch, S. Kreher, B. Schlott, A. Y. Pierik, G. Diekert, *J. Bacteriol.* **2009**, *191*, 588–599.
[23] S. E. Hennig, J.-H. Jeoung, S. Goetzl, H. Dobbek, *Proc. Natl. Acad. Sci. USA* **2012**, *109*, 5235–5240.
[24] M. Sperfeld, G. Diekert, S. Studenik, *Mol. Microbiol.* **2014**, *92*, 598–608.
[25] S. E. Hennig, S. Goetzl, J.-H. Jeoung, M. Bommer, F. Lendzian, P. Hildebrandt, H. Dobbek, *Nat. Commun.* **2014**, *5*, 4626.
[26] W. Buckel, J. W. Kung, M. Boll, *ChemBioChem* **2014**, *15*, 2188–2194.
[27] M. Boll, G. Fuchs, *Eur. J. Biochem.* **1995**, *234*, 921–933.
[28] W. Buckel, M. Hetzel, J. Kim, *Cu. Op. Chem. Biol.* **2004**, *8*, 462–467.
[29] D. M. Smith, W. Buckel, H. Zipse, *Angew. Chem. Int. Ed.* **2003**, *42*, 1867–1870; *Angew. Chem.* **2003**, *115*, 1911–1915.
[30] J. Kim, D. J. Darley, W. Buckel, A. J. Pierik, *Nature* **2008**, *452*, 239–242.
[31] W. Buckel, *Angew. Chem. Int. Ed.* **2009**, *48*, 6779–6787; *Angew. Chem.* **2009**, *121*, 6911–6920.
[32] J. Kim, A. J. Pierik, W. Buckel, *ChemPhysChem* **2010**, *11*, 1307–1312.

[33] S. H. Knauer, W. Buckel, H. Dobbek, *Biochemistry* **2012**, *51*, 6609–6622.
[34] K. P. Locher, M. Hans, A. P. Yeh, B. Schmid, W. Buckel, D. C. Rees, *J. Mol. Biol.* **2001**, *307*, 297–308.
[35] S. H. Knauer, W. Buckel, H. Dobbek, *J. Am. Chem. Soc.* **2011**, *133*, 4342–4347.
[36] J. Kim, M. Hetzel, C. D. Boiangiu, W. Buckel, *FEMS Microbiol. Rev.* **2004**, *28*, 455–468.
[37] M. Hans, W. Buckel, E. Bill, *Eur. J. Biochem.* **2000**, *267*, 7082–7093.
[38] W. Thamer, I. Cirpus, M. Hans, A. J. Pierik, T. Selmer, E. Bill, D. Linder, W. Buckel, *Arch. Microbiol.* **2003**, *179*, 197–204.
[39] M. Hans, W. Buckel, E. Bill, *Journal of Biological Inorganic Chemistry* **2008**, *13*, 563–574.
[40] J.-H. Jeoung, H. Dobbek, *Proc. Natl. Acad. Sci. USA* **2018**, *115*, 2994–2999.
[41] J. A. Gerlt, J. T. Bouvier, D. B. Davidson, H. J. Imker, B. Sadkhin, D. R. Slater, K. L. Whalen, *Biochim. Biophys. Acta* **2015**, *1854*, 1019–1037.
[42] R. Saito, M. E. Smoot, K. Ono, J. Ruscheinski, P.-L. Wang, S. Lotia, A. R. Pico, G. D. Bader, T. Ideker, *Nat. Methods* **2012**, *9*, 1069–1076.
[43] T. D. P. Stack, M. J. Carney, R. H. Holm, *J. Am. Chem. Soc.* **1989**, *111*, 1670–1676.
[44] Y. Nicolet, C. Piras, P. Legrand, C. E. Hatchikian, J. C. Fontecilla-Camps, *Structure* **1999**, *7*, 13–23.
[45] J. W. Peters, W. N. Lanzilotta, B. J. Lemon, L. C. Seefeldt, *Science* **1998**, *282*, 1853–1858.
[46] T. I. Doukov, T. M. Iverson, J. Seravalli, S. W. Ragsdale, C. L. Drennan, *Science* **2002**, *298*, 567–572.
[47] C. Darnault, A. Volbeda, E. J. Kim, P. Legrand, X. Vernède, P. A. Lindahl, J. C. Fontecilla-Camps, *Nat. Struct. Biol.* **2003**, *10*, 271–279.
[48] V. Svetlitchnyi, H. Dobbek, W. Meyer-Klaucke, T. Meins, B. Thiele, P. Römer, R. Huber, O. Meyer, *Proc. Natl. Acad. Sci. USA* **2004**, *101*, 446–451.
[49] B. R. Crane, L. M. Siegel, E. D. Getzoff, *Science* **1995**, *270*, 59–67.
[50] E. N. Mirts, I. D. Petrik, P. Hosseinzadeh, M. J. Nilges, Y. Lu, *Science* **2018**, *361*, 1098–1101.
[51] C. P. Owens, F. E. H. Katz, C. H. Carter, V. F. Oswald, F. A. Tezcan, *J. Am. Chem. Soc.* **2016**, *138*, 10124–10127.
[52] J. W. Peters, M. H. B. Stowell, S. M. Soltis, M. G. Finnegan, M. K. Johnson, D. C. Rees, *Biochemistry* **1997**, *36*, 1181–1187.
[53] D. Sippel, M. Rohde, J. Netzer, C. Trncik, J. Gies, K. Grunau, I. Djurdjevic, L. Decamps, S. L. A. Andrade, O. Einsle, *Science* **2018**, *359*, 1484–1489.
[54] D. Sippel, O. Einsle, *Nat. Chem. Biol.* **2017**, *13*, 956–960.
[55] T. Spatzal, M. Aksoyoglu, L. Zhang, S. L. A. Andrade, E. Schleicher, S. Weber, D. C. Rees, O. Einsle, *Science* **2011**, *334*, 940.
[56] T. Spatzal, K. A. Perez, O. Einsle, J. B. Howard, D. C. Rees, *Science* **2014**, *345*, 1620–1623.
[57] J. T. Kaiser, Y. Hu, J. A. Wiig, D. C. Rees, M. W. Ribbe, *Science* **2011**, *331*, 91–94.
[58] J. B. Howard, D. C. Rees, *Chem. Rev.* **1996**, *96*, 2965–2982.
[59] C. C. Lee, M. A. Blank, A. W. Fay, J. M. Yoshizawa, Y. Hu, K. O. Hodgson, B. Hedman, M. W. Ribbe, *Proc. Natl. Acad. Sci. USA* **2009**, *106*, 18474–18478.
[60] C. C. Lee, Y. Hu, M. W. Ribbe, *Proc. Natl. Acad. Sci. USA* **2012**, *109*, 6922–6926.
[61] D. L. Gerlach, D. Coucouvanis, J. Kampf, N. Lehnert, *Eur. J. Inorg. Chem.* **2013**, *2013*, 5253–5264.
[62] T. Terada, T. Wakimoto, T. Nakamura, K. Hirabayashi, K. Tanaka, J. Li, T. Matsumoto, K. Tatsumi, *Chem. Asian J.* **2012**, *7*, 920–929.

Manuscript received: January 13, 2020
Revised manuscript received: February 14, 2020
Accepted manuscript online: March 18, 2020
Version of record online: March 30, 2020